http://dx.doi.org/10.5012/bkcs.2013.34.5.1391

Homogeneously Dispersed Silver Nanoparticles on the Honeycomb-Patterned Poly(*N*-vinylcarbazole)-cellulose triacetate Composite Thin Films by the Photoreduction of Silver Nitrate

Kwang Il Kim, C. Basavaraja, and Do Sung Huh*

Department of Chemistry and Nanosystem Engineering, Institute of Basic Science, Inje University, Kyungnam 621-749, Korea
**E-mail: chemhds@inje.ac.kr*
Received November 22, 2012, Accepted February 7, 2013

The photocontrolled reduction of silver nitrate to silver (Ag) nanoparticles on honeycomb-patterned poly(*N*-vinylcarbazole) (PVK)-cellulose triacetate (CTA) composite thin films was studied. The composites were prepared *via* the oxidative polymerization of *N*-vinylcarbazole with ferric chloride using different CTA concentrations. A honeycomb-patterned film was fabricated by casting the composite solution under humid conditions. Ag particles with a homogeneous distribution were produced by the composite film in a moderate CTA concentration, whereas aggregated Ag was obtained from the pure PVK film.

Key Words : Photocontrolled reduction, Poly(*N*-vinylcarbazole), Silver nanoparticles, Cellulose triacetate, Honeycomb-patterned film

Introduction

Composite thin films consisting of nanometer-sized metals or semiconductor particles dispersed in solid dielectric materials, such as polymers or glass, have attracted great interest in recent years.[1] Silver (Ag) is a typical material for metal nanoparticles because it has a high optical excitation efficiency and a strong third-order nonlinear optical susceptibility $x^{(3)}$.[2] Ag-dispersed polymers are highly preferred because the resulting nanocomposites can be used in catalysts, drugs and wound dressings, optical information storage, and surface-enhanced Raman scattering.[3-5] However, the formation of homogeneously dispersed Ag nanoparticles on a polymer matrix is difficult because the nanoparticles easily agglomerate.[6] Convenient and effective ways of preparing homogeneously dispersed Ag nanoparticles on polymer materials have yet to be established.

Along with composite thin polymer films with dispersed nanometer-sized metal particles, dimensionally organized matrix structures with highly ordered porous polymer films have also attracted increasing interest because of their potential applications in chemistry, biology and other life sciences, and material technology. Among the many fabrication methods for porous polymer films,[7,8] breath figure formation is a simple and useful technique because highly ordered polymer films are easily produced by evaporating a polymer solution dissolved in a volatile solvent under humid conditions.[9,10] Water vapor condenses on the cooling surface because of rapid solvent evaporation to produce water droplets, which are then trapped on the solution surface *via* surface tension.[11,12]

Poly(*N*-vinylcarbazole) (PVK) has emerged as one of the most useful polymers for electro-optically active applications, including light-emitting diodes and xerography.[13,14] The chemical and thermal stabilities of PVK, combined with its excellent electrical properties, can produce useful electronic devices.[15] Moreover, PVK is considered an ideal model of a non-conjugated photoconducting polymer with strong electron-donor properties.[16] It can stabilize electron-deficient centers *via* the resonance of the nonbonding electron pair on the nitrogen atom in its carbazole ring[17] to reduce the metal cations to metal particles. However, the major limitations of PVK are its unprocessability and intractability, which have made the processing of this material into desired forms rather challenging.

In this aspect, the importance of biodegradable cellulose materials, such as cellulose triacetate (CTA), has been acknowledged in various industries. Furthermore, CTA has the highest thermal stability among all cellulose esters.[18] CTA is used in a wide range of applications, including hemodialysis, reverse osmosis membranes, and liquid crystal displays.[19-21]

The present study proposes a method for the preparation of homogeneously dispersed Ag nanoparticles on the honeycomb-patterned PVK-CTA composite thin film by the photoreduction of silver nitrate. Honeycomb-patterned thin films were fabricated by casting the composite solution under humid conditions. The polymer composites were prepared *via* the polymerization of *N*-vinylcarbazole in the presence of different biopolymer CTA concentrations. CTA was added to improve the mechanical properties of PVK and to control the photoreduction by inhibiting the aggregation of reduced silver nanoparticles on the patterned PVK film.

Experimental

Materials. All reagents, including *N*-vinylcarbazole (98%), CTA, iron(III) chloride hexahydrate (97%), chloroform (≥ 99.8%), and methanol (≥ 99.8%), were purchased from

Sigma-Aldrich Co. (St. Louis, USA) and used as received, without further purification. *N*-vinylcarbazole was used as the monomer, and $FeCl_3$ was used as the oxidizing agent. De-ionized water was used for the experiments.

Preparation of PVK-CTA Composites. Experimental details regarding on the synthesis and characterization of PVK-CTA (PC) composites are described in our previous report.[22] Different concentrations (10, 30, and 50 wt %) of CTA were initially dissolved with the *N*-vinylcarbazole monomer in 10 mL chloroform, and the mixture was sonicated for 1 h. In a separate mixture, 1 g of oxidizing agent was added to 10 mL chloroform, and the mixture was filtered. The filtrate was slowly added to the solution containing CTA and the monomer. Afterwards, the mixture was sonicated for ~10 min and refrigerated at a maintained temperature range of 0 °C to 4 °C for ~12 h. Methanol was added to the mixture when the suitable temperature had been achieved, and a white precipitate was obtained. The precipitate was washed several times with distilled methanol and water and dried in an oven for ~24 h at 80 °C. For comparison, pure PVK was also synthesized without CTA using the same procedure. The CTA concentrations used in the polymerization of *N*-vinylcarbazole were 10, 30, and 50 wt %. The resulting composites are hereafter abbreviated as PC-10, PC-30, and PC-50, respectively, as shown in Figure 1(a).

Synthesized PVK-CTA composites were further characterized by FTIR and UV-vis spectroscopy to determine the successful formation of the polymer composites. The infrared spectra of the polymer samples pelletized with KBr were obtained using an FTIR spectrometer (Perkin-Elmer Model 1600). Approximately 60 scans were signal-averaged at a resolution of 2 cm^{-1} from 4000 cm^{-1} to 400 cm^{-1}. The UV-vis spectra of the PVK and PC polymer composites (0.05 g in 10 mL chloroform) were recorded using a Shimadzu UV-Vis near-infrared spectrophotometer (UV-3101PC).

Fabrication of Honeycomb-Patterned Thin Film and Photoreduction of $AgNO_3$. The fabrication of honeycomb-patterned thin films was performed by the similar process introduced in our previous reports,[23,24] however, a highly ordered honeycomb-patterned film was obtained without the amphiphilic copolymer to stabilize the air-water interface in this case.[24] A honeycomb-patterned film 1.8 × 1.8 cm^2 in size was prepared and placed on a Petri dish with a diameter of 3.0 cm, and 6 ml of 0.1 M or 1.0 M $AgNO_3$ solution was poured onto the dish. UV light was vertically illuminated onto the dish using a Xe-Hg lamp (L9588 series, Hamamatsu Co.) ranging from 250 nm to 500 nm. The light intensity on the solution surface was adjusted to ~0.2 mW/cm^2.

Figure 1(b) illustrates the overall experimental scheme reducing $AgNO_3$ solution by UV illumination. The Ag-

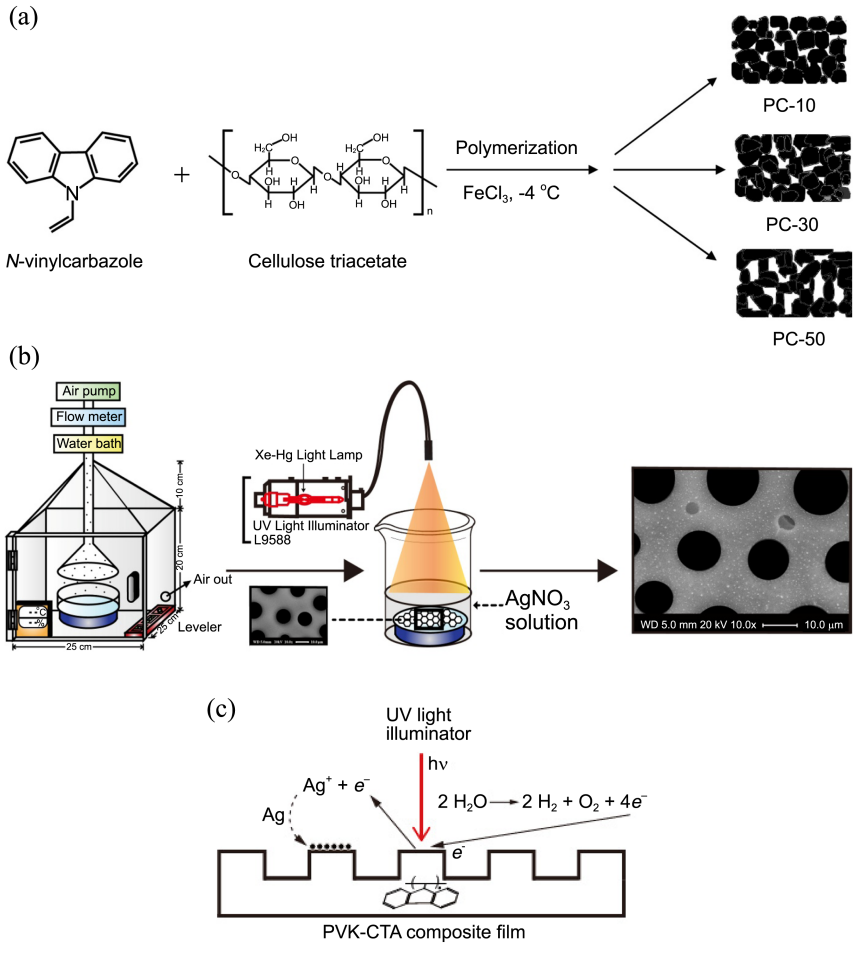

Figure 1. Overall experimental scheme for the photoreduction of $AgNO_3$ on honeycomb-patterned PVK-CTA composite films.

metallized honeycomb-patterned thin films were analyzed using a scanning electron microscope (SEM, Philips XL-30).

Results and Discussion

Characterization of Synthesized PVK-CTA Composites. Figure 2(a) shows the FTIR spectra of PVK, CTA, as well as those of the PC-10, PC-30, and PC-50 composites in the regions between 500 and 4000 cm^{-1}. The spectra obtained for the PVK and the PC polymer composites are consistent with the infrared PVK spectra reported previously.[25-27]

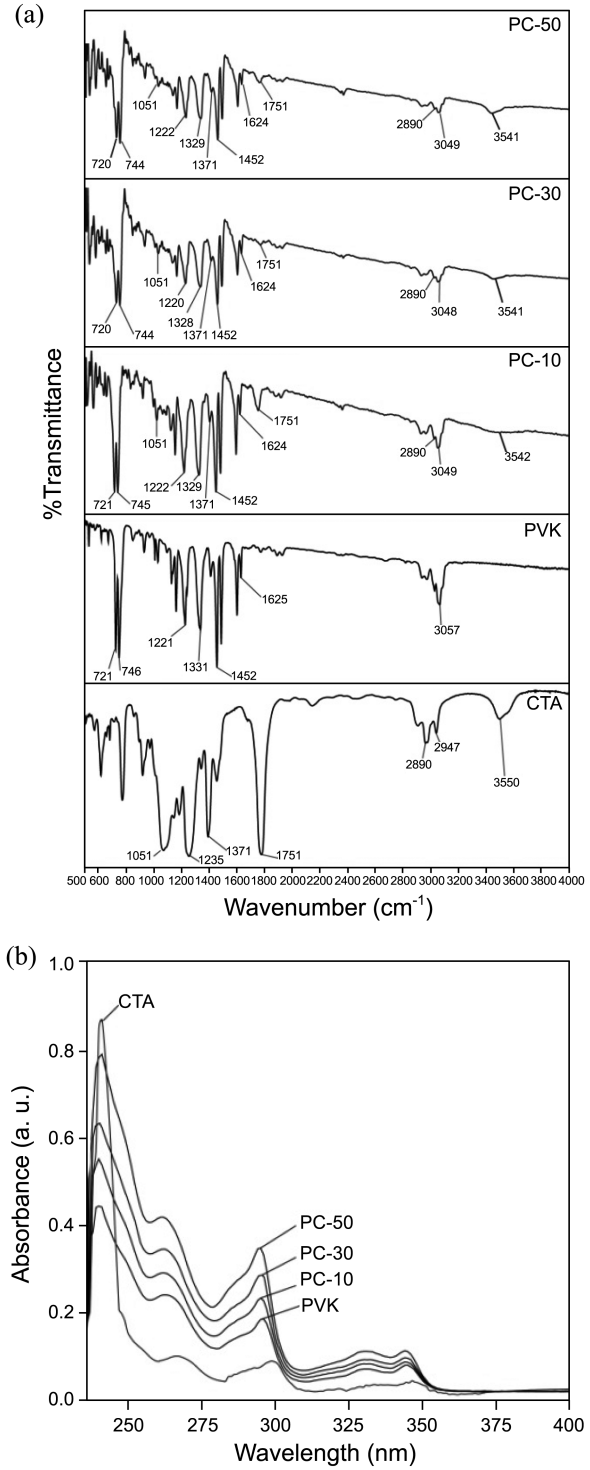

Figure 2. Characterization of synthesized PVK, CTA, and PVK-CTA composites. (a) FTIR and (b) UV-vis spectra.

The spectra given in Figure 2(a) further provide evidence on the formation of the PVK moiety. Table 1 summarizes the major FTIR peaks observed for PVK, CTA, and the PC polymer composites, along with their probable assignments. The presence of PVK in the PC polymer composites was supported by the appearance of FTIR peaks at 721, 745, 1220, 1331, 1452, 1625, and 3057 cm^{-1} in the region between 500 and 4000 cm^{-1}. The CTA transmission band located around 1751 cm^{-1} is attributed to the stretching vibrations of the carbonyl group.[28] The bands at 1219 and 1055 cm^{-1} correspond to the stretching modes of the C–O single bonds. The transmission bands at 2947 and 2890 cm^{-1} are assigned to the C–H bonds, and the wide band detected at 3541 cm^{-1} is assigned to the O–H stretching modes.

Figure 2(b) shows the UV-vis spectra of PVK, CTA, PC-10, PC-30, and PC-50. All the absorbance peaks observed at approximately 240, 262, 295, 320, and 340 nm are similar to the PVK peaks reported previously.[25] In a similar fashion, CTA exhibited two absorbance bands at 240 and 300 nm. Note that the UV-vis spectra of the PC-10, PC-30, and PC-50 polymer composites show all the absorbance bands pertaining to PVK and CTA. The peaks exhibited by the PC polymer composites show only slight blue shifts of approximately 2 nm to 5 nm between 260 and 295 nm. This shift in the absorbance bands of the polymer composites may be attributed to the interactions between CTA and the PVK polymer.

Photoreduction of $AgNO_3$ on the Honeycomb-Patterned Composite Film. Figures 3(a) and 3(b) show typical SEM images of the patterned films of pure CTA and PVK, respectively, by UV illumination after the reduction of $AgNO_3$. For the photoreduction, 0.1 M $AgNO_3$ solution was illuminated for 10 min with a 0.2 mW/cm^2 light source. The magnified images in the insets clearly illustrate the results of photoreduction on the patterned film. Figure 3(a) shows the absence of Ag particles on the film indicates that no photoreduction occurred at all on the CTA film. Meanwhile, Figure 3(b) shows the results of photoreduction observed on the patterned PVK film, which was completely eliminated by agglomerated silver. These findings indicate that obtaining homogeneously well-dispersed Ag nano-particles on the films of pure CTA and PVK are impossible because photoreduced Ag was not obtained in CTA, whereas an overproduction of photoreduced Ag occurred in the PVK film.

Figures 4(a)-(c) show typical SEM images of patterned films after the reduction of $AgNO_3$ by UV illumination in the PVK-CTA composites of PC-10, -30, and -50, respectively, on 0.1 M $AgNO_3$ solution for 10 min. Considering the structure of the honeycomb-patterned film with pure PVK or CTA film shown in Figure 3, the patterns obtained in the composites indicate better-ordered patterns with a consistent pore size and distance between the pores (Figure 4). The formation of a highly ordered honeycomb pattern by the

Table 1. Summary of the major FTIR peaks observed for PVK, CTA, and PC polymer composites along with their probable assignments

Assignments	Observed peaks (cm^{-1}) for				
	PVK	CTA	PC-10	PC-30	PC-50
Ring deformation of substituted aromatic structure			721	720	720
> CHβ rocking vibration			745	744	744
Out of plane deformation of vinylidene group	721		1222	1220	1222
> CH_2 deformation of vinylidene group	746		1329	1328	1329
Ring vibration of *N*-vinylcarbazone moiety	1221		1452	1452	1452
C=C stretching vibration of vinylidene group	1331		1624	1624	1624
Aromatic C-H stretching vibration	1452		3049	3048	3049
Stretching vibrations of C=O	1625	1751	1751	1751	1751
Stretching vibrations of C–H	3057	2947	–	–	–
		2890	2890	2890	2890
Stretching modes of O–H		3541	3542	3541	3541

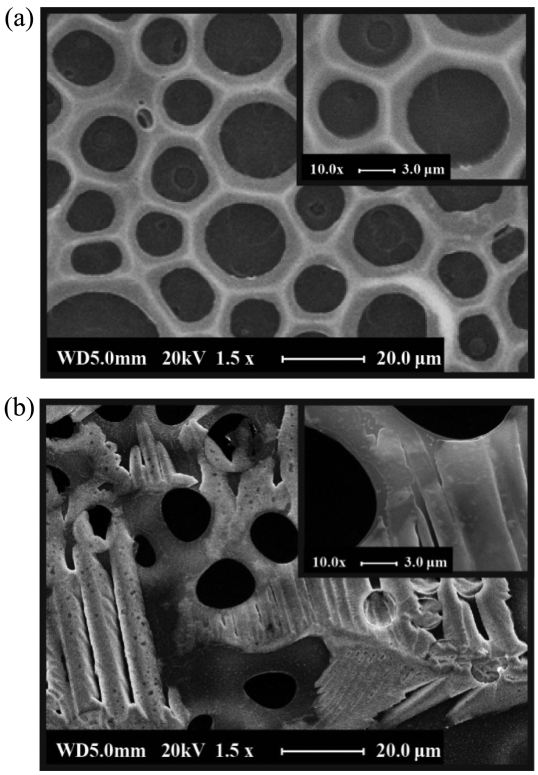

Figure 3. Typical SEM images of honeycomb-patterned films after photoreduction for 10 min illumination time with 0.1 M $AgNO_3$ solution: (a) pure CTA, (b) pure PVK. The insets show the magnified images.

PVK-CTA composite polymers without an amphiphilic co-polymer can be attributed to the complementary effect of CTA as an amphiphilic component to the hydrophobic PVK polymer.

Apart from the results obtained with the PVK and CTA films, Ag particles were obtained by photoreduction in the composite films, as shown in Figures 4(a)-(c). However, the size and homogeneity of the particles depended on the concentration of CTA added. Homogeneously distributed nanometer-sized Ag particles were obtained with PC-10 and PC-30, as shown in Figures 4(a) and 4(b). However, the

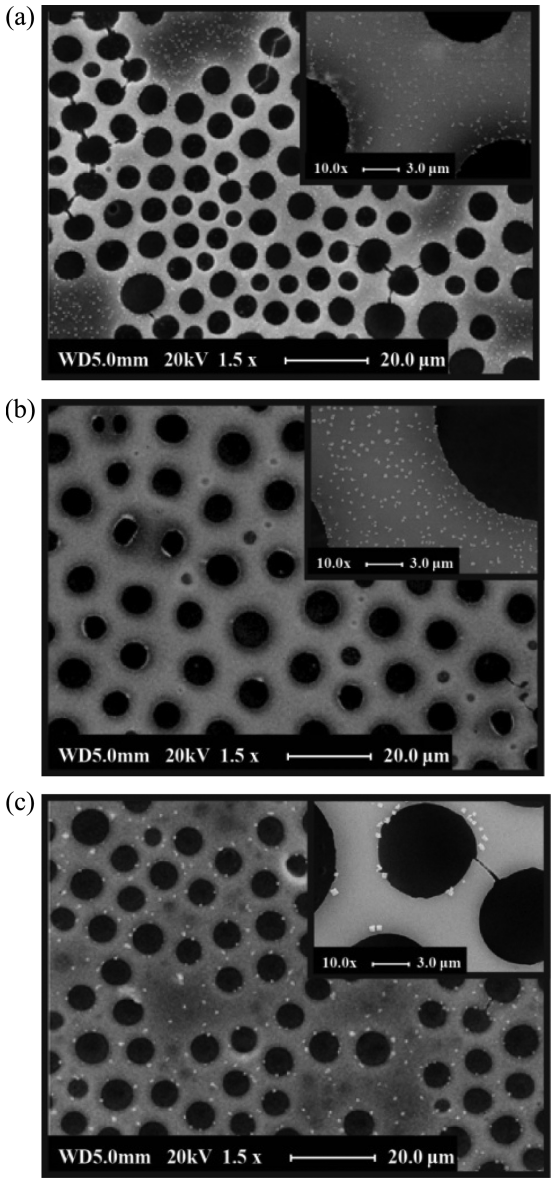

Figure 4. Typical SEM images of honeycomb-patterned films after photoreduction in the composite films obtained by 10 min illumination in 0.1 M $AgNO_3$ solution. (a) PC-10, (b) PC-30, and (c) PC-50, respectively. The insets show the magnified images.

magnified inset images in these figures display a small difference in the size of Ag particles between the two films, in which smaller-sized and better-dispersed Ag particles were obtained with the PC-30 film. The increased incorporation of CTA into the PC-50 composite, however, caused a rather contrary effect in the PC-50 film, as shown in Figure 4(c), in which photoreduced silver particles were sparsely distributed and the size of particles was increased. These experimental results indicate that the amount of CTA in the composite acted as a controller, moderating the effect on the photoreduction of $AgNO_3$ induced by the PVK polymer in the composite. Therefore, we can suggest the process for the photoreduction of Ag^+ to Ag on the patterned film described in Figure 1(c) as follows:

$$PVK \rightarrow PVK^+ + e^- \quad (1)$$

$$Ag^+ + e^- \rightarrow Ag \quad (2)$$

$$2H_2O \rightarrow 2H_2 + O_2 + 4e^- \quad (3)$$

$$PVK^+ + e^- \rightarrow PVK \quad (4)$$

Photoreduction was thus initiated by the donation of electrons from PVK by the resonance involving the nonbonding electron pair on the nitrogen atom in the PVK carbazole ring. Therefore, the photoreduction was not facilitated by the PC-50 film containing comparatively high CTA concentrations.

Effects of Illumination Time and Concentration of $AgNO_3$. Figure 5 shows the effects of the illumination time and $AgNO_3$ concentration on photoreduction. Figures 5(a)-(c) show typical SEM images of reduced Ag particles on the PC-10, -30, and -50 composite films, respectively, with a doubled illumination time of 20 min, under otherwise equal experimental conditions to those for Figure 4. In comparison with the results obtained in Figure 4, we can easily see that the sizes of the Ag particles obtained on the patterned films were increased in all the three films, PC-10, PC-30, and PC-50, and that the Ag particles were not evenly distributed because of aggregation. Thus, a longer period of illumination can produce a larger number of Ag seed particles on the patterned film, thereby increasing the size of seed particles by aggregation. Furthermore, the illumination time is also very significant in the formation of homogeneously dispersed Ag nanoparticles on the PVK composite film.

Figures 5(d)-(f) show typical SEM images of reduced Ag particles on the PC-10, PC-30, and PC-50 composite films, respectively, obtained using the same experimental conditions used for Figure 4, except for the $AgNO_3$ concentration. The concentration was increased from 0.1 M to 1.0 M to examine the effect of aqueous $AgNO_3$ concentration on photoreduction. Despite the same illumination time of 10 min, lumped particles were also produced together with small Ag particles. The lumps formed were more visible in the PC-10 and PC-30 films, as shown in Figures 5(d) and 5(e). The lumps can be ascribed to the higher PVK composition, which acted as a reducing agent. This explanation is supported by the SEM image Figure 5(f) of PC-50, in which formation of the lump is not so severe compared with the films of PC-10 and PC-30.

Figure 6 shows a diagram summarizing the size distributions of the Ag particles on the PC-10, PC-30, and PC-50 patterned films, depending on the illumination time, at 0.1 M $AgNO_3$ concentration. The diagram shows that the increase in the illumination time increased the range of distribution of the Ag particle size, regardless of the type of composite film,

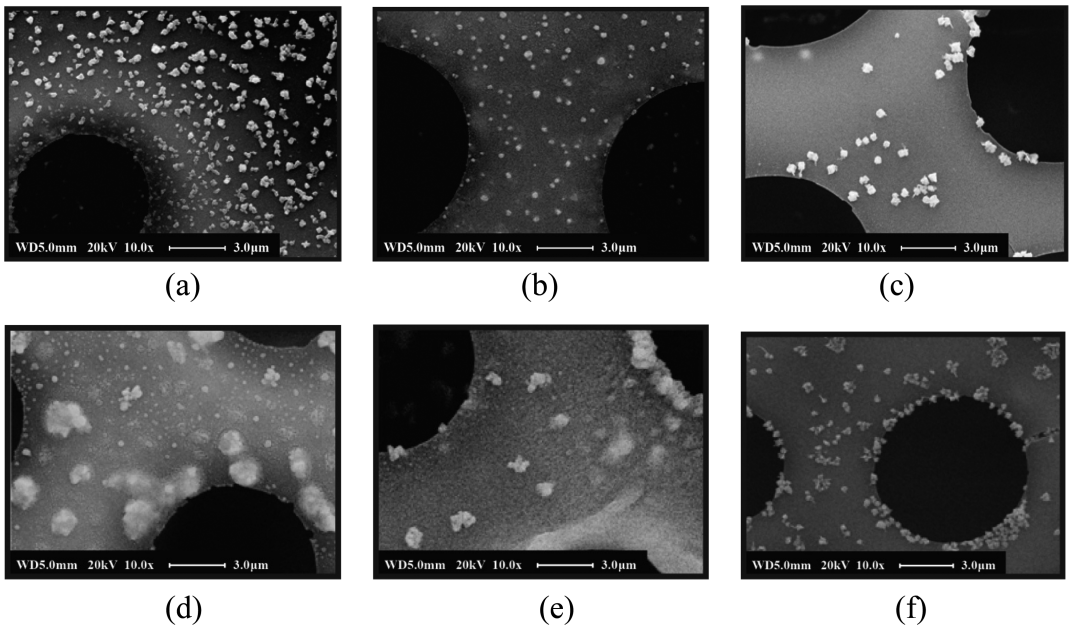

Figure 5. Typical SEM images of the reduced Ag particles under slightly adjusted experimental conditions. (a) PC-10, (b) PC-30, and (c) PC-50 were obtained by doubling the illumination time to 20 min under otherwise identical experimental conditions; (d) PC-10, (e) PC-30, and (f) PC-50 were obtained by increasing the $AgNO_3$ solution concentration from 0.1 M to 1.0 M under otherwise identical experimental conditions.

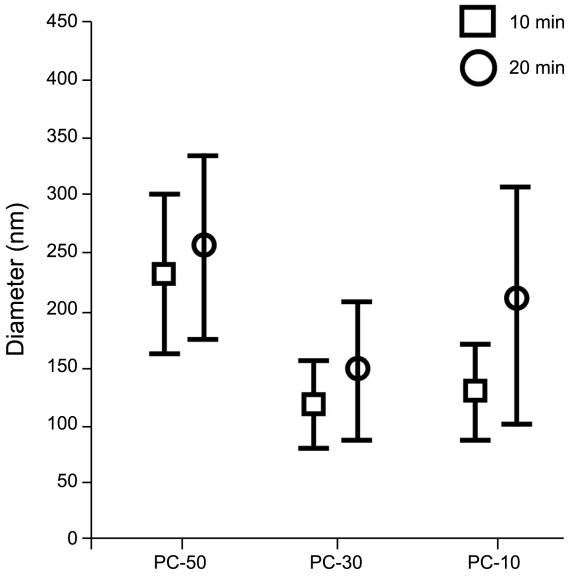

Figure 6. Diagram showing the distribution of the particle size obtained at illumination times of 10 and 20 min, at 0.1 M $AgNO_3$.

which can be ascribed to the increased number of Ag seed particles being aggregated by accumulation, which thus caused significant variation in the sizes of particles. Among the three composite films, the PC-30 film showed the lowest range in the distribution of particle sizes at both 10 and 20 min illumination time. Therefore, a more homogeneous distribution of Ag nanoparticles was achieved by the composite film with a moderate CTA concentration. Therefore, the biopolymer of CTA can be effectively used for the photoreduction of PVK film by enhancing the reduction efficiency to form homogeneously dispersed Ag nanoparticles without aggregation, thereby making the PC composite cost-effective and mechanically stable.

Conclusion

The effect of UV illumination on the reduction of silver ions on the surface of honeycomb-patterned PVK-CTA composite films was investigated. The CTA concentration in the composite was varied from 10, 30, and 50 wt %. The structure of the honeycomb pattern of the composite films and the adsorption morphology of silver particles on the films were found to depend on the concentration of CTA in the composite. The sizes of reduced silver particles increased with increasing $AgNO_3$ concentration and a long period of illumination. However, the aggregation of silver nanoparticles occurred under higher concentration and at a longer illumination period, and Ag particles with a highly homogeneous distribution were obtained using composite films with moderate CTA concentrations.

Acknowledgments. This research was supported by 2013 Inje University Research Grant. Prof. Huh is grateful to Prof. Kozo Kuchitsu for providing helpful comments on the manuscript.

References

1. Yang, B.; Yoon, K.; Chung, K. *Mater. Chem. Phys*. **2004**, *83*, 334.
2. Moskovits, M. *Rev. Mod. Phys.* **1985**, *57*, 783.
3. Son, W. *Macromol. Rapid. Commun*. **2004**, *25*, 1632.
4. Doty, R. C.; Tshikhudo, T. R.; Brust, M.; Ferning, D. G. *Chem. Mater.* **2005**, *17*, 4630.
5. Liu, H.; Ge, X.; Ni, Y.; Ye, Q.; Zhang, Z. *Radiat. Phys. Chem*. **2001**, *61*, 89.
6. Ghosh, K.; Maiti, S. N. *Appl. Polym. Sci.* **1996**, *60*, 323.
7. Wang, D. Y.; Caruso, F. *Adv. Mater.* **2001**, *13*, 350.
8. Wilbur, J. L.; Biebuyck, H.; MacDonald, J. C.; Whitesides, G. M. *Langmuir.* **1995**, *11*, 825.
9. Francois, B.; Pitois, O.; Françoi, J. *Adv. Mater.* **1995**, *7*, 1041.
10. Karthaus, O.; Maruyama, N.; Cieren, X.; Shimomura, M.; Hasegawa, H.; Hashimoto, T. *Langmuir.* **2000**, *16*, 6071.
11. Maruyama, N.; Koito, T.; Nishida, J.; Sawadaishi, T.; Cieren, X.; Ijiro, K.; Karthaus, O.; Shimomura, M. *Thin Solid Films*. **1998**, *327*, 854.
12. Yabu, H.; Shimomura, M. *Langmuir*. **2006**, *22*, 4992.
13. Nalwa, H. S. *Handbook of Nanostuctured Materials and Nanotechnology*; Academic Press: New York, 2000.
14. Malinauskas, A.; Malinauskiene, J.; Ramanavicius, A. *Nanotechnology* **2005**, *16*, R51.
15. Bhadra, S.; Singha, N. K.; Khastgir, D. *Synth. Met*. **2006**, *156*, 1148.
16. He, G.; Chang, S. C.; Chen, F. C.; Li, Y.; Yang, Y. *Appl. Phys. Lett*. **2002**, *81*, 1509.
17. Penwell, R. C.; Ganguly, B. N.; Smith, T. W. *J. Polym. Sci. Macromol*. **1978**, *13*, 63.
18. De Smet, R.; Dhondt, A.; Eloot,S.; Galli, F.; M. Watrloos, A.; Vanholder, R. *Nephrol. Dial. Transplant*. **2007**, *22*, 2006.
19. Kastelan, K. L.; Dananic, V.; Kunst, B.; Kosutic, K. *J. Membrane Sci.* **1996**, *109*, 223.
20. Arous, O.; Amara, M.; Kerdjoudj, H. *J. Appl. Polym. Sci.* **2004**, *93*, 1401.
21. Derbal, A.; Omeiri, S.; Bouguelia, A.; Trari, M. *Int. J. Hydrogen Energy* **2008**, *33*, 4274.
22. Basavaraja, C.; Jo, E. A.; Huh, D. S. *Mater. Lett*. **2010**, *64*, 762.
23. Kim, B. S.; Basavaraja, C.; Jo, E. A.; Kim, D. G.; Huh, D. S. *Polymer*. **2010**, *51*, 3365.
24. Kim, D. G.; Basavaraja, C.; Yamaguchi, T.; Huh, D. S. *Polymer*. **2012**, *53*, 1347.
25. Kang, Y. O.; Choi, S. H.; Gopalan, A.; Lee, K. P.; Kang, H. D.; Song, Y. S. *J. Appl. Polym. Sci.* **2006**, *100*, 1809.
26. Ouro-Djobo, S.; Bernede, J. C.; Napo, K.; Guellil, Y. *Mater. Chem. Phys.* **2002**, *77*, 476.
27. He, R.; Qian, X.; Yin, Y.; Bian, L.; Xi, H.; Zhu, Z. *Mater. Lett*. **2003**, *57*, 1351.
28. Gardner, J. S.; Walker, J. O.; Lamb, J. D. *J. Membr. Sci.* **2004**, *229*, 87.